Indian Journal of Pure & Applied Physics
Vol. 58, October 2020, pp. 726-734

Influence of substrate temperature on physical properties of $MnSbInS_4$ thin films prepared by a simplified spray pyrolysis technique for photovoltaic applications

A Kennedy[a*], V Senthil Kumar[b] & K Pradeev raj[a]

[a]Department of Physics, CSI College of Engineering, Ooty – 643 215, India.

[b]Department of Physics & Electronics, Karpagam University, Coimbatore, Tamil Nadu, India.

*Corresponding author (E-mail: kennedycsice@gmail.com)

Received 24 April 2017; accepted 20 July 2017

$MnSbInS_4$ multi-component semiconductor thin films are prepared by chemical spray pyrolysis on glass substrates at various substrate temperatures ranging from 250-400 °C with a constant spray time (5mins). The structural, morphological, optical and electrical properties of the thin films are investigated through different techniques such as X-ray diffraction (XRD), electron diffraction spectroscopy (EDS), UV-Vis absorption spectroscopy and four probe method. The X-ray spectra reveal that the $MnSbInS_4$ films are polycrystalline in nature with a cubic spinel structure having (220) plane as the preferred orientation. The energy dispersive analysis by X-ray (EDS) studies confirm the presence of Mn, In, Sb and S in the film grown at a substrate temperature of 250 °C. Optical measurements allow us to determine the absorption coefficient which is as high as (1.22×10^5 cm^{-1}) at 250 ºC indicating that $MnSbInS_4$ compound has an absorbing property favorable for applications in solar cell devices. It is interesting to note that the structural homogeneity and crystallinity of the films is improved due to the decrease in absorption coefficient (α) and extinction coefficient (k) with an increase of substrate temperature. The observations from photoluminescence measurements reveal that the photoemission is mainly due to the donar-acceptor pair transitions. Moreover, from the electrical studies, it is observed that the electrical resistivity (ρ) is strongly affected by substrate temperature and the lowest resistivity ($\rho = 4.77 \times 10^3$ Ω m) is obtained for the film grown at 400 ºC. Stylus profilometer was used to measure the film thickness and the values range between 768 nm (250 °C) to 617 nm (400 °C). This indicates that, as the substrate temperature increases, the thickness of the film decreases. Other important parameters like micro-strain (ε) and dislocation density (δ) which are commonly used to describe the structural analysis are also presented.

Keywords: $MnSbInS_4$ thin films, Chemical spray pyrolysis, X-ray diffraction, Optical and electrical properties

1 Introduction

In the past decade, extensive research was devoted to growing various kinds of binary[1-3] and ternary[4-6] semiconducting materials. They have potential use in solar cells, optoelectronic devices, photoconductors and infrared detector devices[7,8]. Manganese indium Sulphide ($MnIn_2S_4$) thin films with a wide direct band gap possess semiconducting properties have attracted the attention of many researchers. $MnIn_2S_4$ is an n-type semiconductor with optical band gap energy equal to 3.2 eV that can be modified by adding suitable doping material (or) by changing the concentration of cation or anion in the film[9]. In solar cell systems, the replacement of Cadmium Sulphide (Cds) with a higher band gap of $MnIn_2S_4$ (Eg = 3.2 eV) thin films lead to decrease the window absorption loss and increase the short circuit current[10].

In the recent years, multi-component thin films have been grown by a variety of deposition techniques such as chemical bath deposition[11], thermal evaporation[12], solve thermal synthesis[13], atomic layer chemical vapor deposition[14] and spray pyrolysis[15]. Among them, spray pyrolysis is a desirable method because of its low cost, simplicity, mass production capacity and large area coatings. Further, it has the advantages like ease of adding doping materials, high growth and minimum wastage of the source materials which are very much desirable for many industrial applications[16]. It is to be noted that, physical parameters like the thickness of the film, temperature, deposition rate and spray time strongly influence the physical properties of the films[17]. Spray pyrolysis is an eco-friendly technique in which the above parameters can controlled in an effective manner[18].

Information on structural and optical properties of $MnIn_2S_4$ thin films is provided by R.K. Sharma

*Corresponding author: (E-mail: kennedycsice@gmail.com)

et al[19], but studies relating to electrical properties were not carried widely by researchers[20]. Recently M. Guk *et al*[21]. reported about the structural and photoluminescence properties of $MnIn_2S_4$ crystals. The current study aims to discuss on chemical composition and electrical properties along with structural and optical properties of $MnSbInS_4$ thin films at different substrate temperature. The main objective of this work is to prepare high- quality thin films by spray pyrolysis technique and to obtain maximum transmittance and electrical conductivity which could find wide applications in the field of optoelectronic devices.

2 Materials and Methods

2.1 Material deposition

Aqueous solution of manganese (ll) chloride ($MnCl_2$), indium (lll) chloride ($InCl_3$), thiourea ($CS(NH_2)_2$) and antimony (lll) chloride ($SbCl_3$) are used to deposit $MnSbInS_4$ thin films on glass temperatures. At first, the aqueous solutions (0.1M) of these salts are prepared and then they are mixed thoroughly with appropriate proportions in order to have manganese to indium molar ratio (Mn/In: 1.25) and (Mn+In)/S fixed to 1 in the solutions. The manganese (ll) chloride and indium (lll) chloride are mixed and then thiourea is added. The resulting solution is doped with antimony (lll) chloride ($SbCl_3$) of 0.01M. The solutions are prepared by dissolving in deionized water. The glass substrates (25mm x 25mm x 1mm) are precleaned ultrasonically with organic solvents and deionized water for several times and to remove the contaminations if anything present on the surface of the substrate. The resulting solutions are sprayed on glass substrates, with a solution flow- rate of 1mL/min, and a nozzle to substrate distance of 25 cm. The deposition time is fixed at 5minutes. Compressed air is used as carrier gas for the deposition. The films are deposited at different substrate temperature 250, 300, 350 and 400 °C and the deposited films are allowed to cool slowly to room temperature. The substrate temperature is maintained by a temperature controller and a chromal-alumel thermocouple. The chemicals used in the present work are of analytical grade.

During spray pyrolysis technique, a balanced chemical reaction to from $MnSbInS_4$ thin films could be:

$$MnCl_2 + SbCl_3 + InCl_3 + 4SC(NH_2)_2 + 8H_2O \rightarrow MnSbInS_4 + 8NH_4Cl + 4CO_2 \quad \ldots (1)$$

Since the byproduct NH_4Cl is volatile at the reaction temperature.

2.2 Characterization techniques

The structure of the prepared films is characterized by X-ray diffraction (XRD) in the range of 10°C-80°C with CuKα radiation having wavelength 1.5406 Å operated at 40 KV and 30 m A. The surface morphologies were investigated by Field Emission Scanning Electron Microscope (FESEM) operated at 30KV with a scanning rate of 50 μs. The elemental composition analysis is carried with energy dispersive X-ray spectroscopy (EDS-model: JOEL -JEM 2100). Optical absorbance and transmittance spectra were measured using UV-Vis spectrometer (V-670-JASCO) at room temperature in the wavelength range of 200-2000 nm. Photoluminescence (PL) spectra of the films are recorded using a 350 nm He-Cd laser and a JOBNYUONHR-460 monochromator at room temperature in fluorescence emission scan mode. The electrical conductivity measurements are performed at room temperature by a four-probe method.

3 Results and Discussions

3.1 Structural analysis

The effect of substrate temperature on the X-ray diffraction patterns of the $MnSbInS_4$ thin films is shown in Fig. 1. From the diffraction patterns, strong

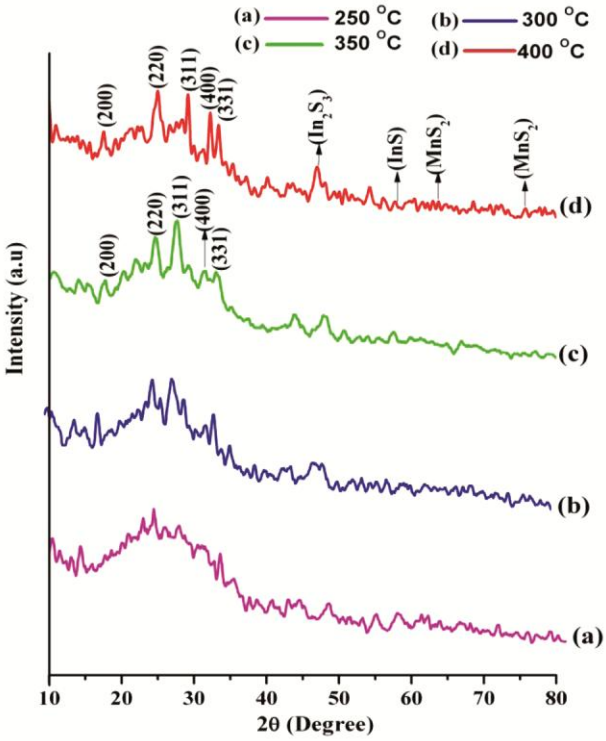

Fig. 1 — X-ray diffraction spectra of $MnSbInS_4$ thin films prepared at various substrate temperatures: (a) 250 °C (b) 300 °C (c) 350 °C (d) 400 °C.

diffraction peaks at 2θ = 23.45°, 27.57° and 33.4° are assigned to (220), (311) and (400) reflecting planes respectively. These diffraction peaks indicate the presence of polycrystalline cubic spinel structure[19]. This is in good agreement with JCPDS data No: 79-1018, 79-1014, 51-1160, 19-0588, 89-3708 and earlier reports[22-25]. The crystal structure of $MnSbInS_4$ has Mn at the octahedral position and In at tetrahedral position[26]. Moreover Mn and In have nearly the same atomic radii 0.91 and 0.92 Å, leading to a high degree of inversion[27]. The small amount (0.01M) of Sb concentration did not alter the cubic spinel structure of the film[28]. It is noted that the intensity of the characteristic peak corresponding to (220) plane increases with an increase of substrate temperature. This may be due to the improvement in the crystallinity of the films at higher deposition temperatures[29]. Further, at higher substrate temperature, the increase in grain- size will reduce the strain and dislocation density (Table 1.), which will greatly improve the crystallinity of the film[18]. Moreover, a few additional peaks are observed which may form due to the formation of intermediate complex compounds such as MnS_2, InS, and In_2S_3 as a result of thermal decomposition of metal chlorides and thiocarbamide[30-32].

The crystallite size (D) is calculated using Scherrer's formula[33]:

$$D = \frac{k\,\lambda}{\beta\ cos\theta} \quad \ldots (2)$$

where, k is a constant taken as 0.9, λ is the X-ray wavelength (1.5406 Å), β is the full width at half maximum (FWHM) of the peak in radian and θ is the diffraction angle.

The average size is calculated and it is found to be in the range between 16.8 and 28.2 nm. The variation of the grain size with respect to substrate temperatures are presented in Table 1. From Table 1, it is clear that the grain size increases with an increase of substrate temperature. This may be due to the improvement in the crystallinity of the films grown at higher substrate temperature[34]. Further, the mobility of the added atoms increases as the substrate temperature increases which result in the increase in grain size and improvement in the crystallinity of the films[35].

Using grain size values, the dislocation density (δ), defined as the length of dislocation lines per unit volume of the crystal is calculated by using the Williamson and Smallman's formula[36].

$$\delta = 1/D^2 \quad \ldots (3)$$

The micro-strain (ε), defined as a measure of the change in the size or shape of a body is referred to its original size or shape developed in the films. The micro-strain (ε), which is an important structural parameter is calculated using the following relation[37].

$$\varepsilon = \beta \cos\theta /4 \quad \ldots (4)$$

where, D is the crystalline size, β is the full-width half maximum in radians and θ is Bragg's diffraction angle. The variation of dislocation density (δ) and microstrain (ε) with substrate temperature (250-400 ºC) are presented in Table. 1. From Table 1, it is clear that the micro-strain and dislocation density of the material of the film decreases with the increase of deposition temperature. This may be due to the increase in particle size and improvement in the stoichiometry of the film grown at higher substrate temperatures[38]. Further, the decrease in the lattice strain with the increase of substrate temperature results in the reduction of lattice imperfections of the grown films[39].

3.2 Elemental composition analysis

The elemental composition and the purity of $MnSbInS_4$ thin films deposited at a substrate temperature of 250°C, is observed from the energy dispersive spectrum (EDS) is shown in Fig. 2 and Table. 2. The EDS spectrum indicates the presence of elements such as manganese (Mn), indium (In), sulphur (S) and antimony (Sb) in the deposited thin films. It is noted that, the oxygen content is present in the $MnSbInS_4$ films deposited at a substrate temperature of 250ºC. The oxygen content is not only chemisorbed in the film[40], but also an oxygen-containing phase is formed during the film growth.

The oxygen atoms diffuse through the grain boundaries of the film without any chemical reaction.

Table 1 — Micro structural parameters of $MnSbInS_4$ thin films formed at different substrate temperatures.

Substrate Temperature (°C)	Bragg's angle (2θ) degree	Particle size (nm) (D)	Dislocation density lines/m^2 (δ) 10^{15}	Strain ε 10^{-3}
250	29.14	16.80	3.543	2.115
300	33.12	22.12	2.043	1.673
350	33.25	23.03	1.885	1.463
400	34.89	28.20	1.257	1.364

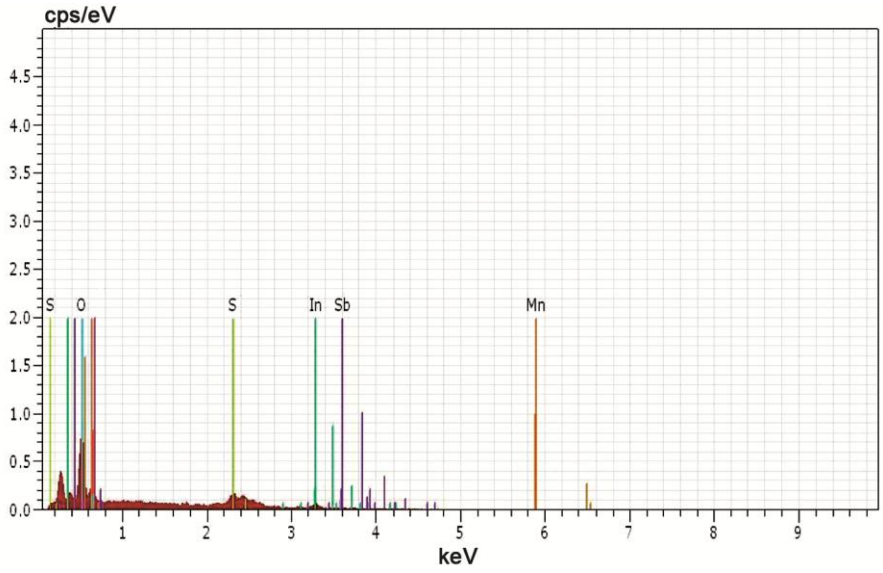

Fig. 2 — EDS spectra of the $MnSbInS_4$ films prepared at 250 °C

Table 2 — Elemental Composition of $MnSbInS_4$ thin films deposited at 250 ºC.

Element	Atomic %	Weight %
Mn	18.74	18.34
In	20.87	17.03
S	11.23	11.51
Sb	12.34	10.93
O	36.82	42.19

These atoms are bounded at the surface and grain boundaries and they do not enter into the crystallites[41]. Hence, the properties of the films are not altered by oxygen content. Further, an intense peak of Silicon (Si) is observed which indicates that the film is deposited on a glass substrate and no trace of foreign elements is identified from the EDS analysis.

3.3 Optical Studies

The substrate temperature- influenced change in transmission spectra of $MnSbInS_4$ thin films recorded in the wavelength range 300-1500 nm is presented in Fig. 3.

From the transmittance spectra, the lower transmittance is observed in the UV region, while in the visible (VIS) and infrared (IR) regions high transmittance is observed. Our results are in good agreement with the results obtained by Patil *et al.*[42]. The high transparency in the visible (VIS) and infrared (IR) regions is a consequence of the wide band gap of the film[43]. On the other hand, the low transmittance in the UV region is an indication that at lower wavelengths there is no transmission because all the light is absorbed. For higher wavelengths

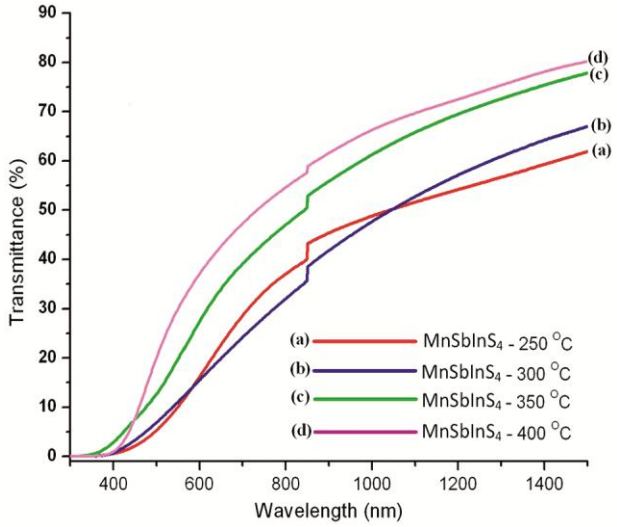

Fig. 3 — Transmittance spectra of $MnSbInS_4$ films sprayed at various substrate temperatures: (a) 250°C (b) 300°C (c) 350°C (d) 400°C

region, however, there are no appropriate electronic transitions possible so transmission is very high in this range[44]. Materials having low absorbance and low reflectance in the visible region makes the thin film as a suitable antireflection layer in solar cells working mainly in the visible region[45]. Further, the semiconductor thin films are used as thermal imaging camera in photo thermal industries.

From the transmittance spectra, it is also noted that an increase in the optical transmittance property is observed at a higher substrate temperature (80% at 400 °C)[46]. The improved transmittance with escalating substrate

Table 3 — Optical parameters of $MnSbInS_4$ sprayed at different substrate temperatures.

Temperature (°C)	Film Thickness (nm)	Transmittance T (%)	Absorption coefficient α 10^5 (cm^{-1})	Extinction coefficient K
250	768	62	1.22	0.48
300	726	67	1.03	0.41
350	664	78	0.84	0.33
400	617	80	0.78	0.31

temperature enhances improvement in structural homogeneity and better crystallinity[41]. Moreover, at higher substrate temperatures the optical scattering diminishes and thus leads to the enhancement of optical transmission[47]. From our previous reports, it is noted that for pure $MnIn_2S_4$ films, the optical transmittance is about 75%[48]. But for $MnSbInS_4$ thin films, the optical transmittance is about 80 %. The transmission is higher in the doped $MnIn_2S_4$ film compared with an undoped thin film. In general, while doping the grain size is reduced, thus results in the improvement in the optical property of the thin films[49]. The doped Sb content has a great effect on the transmission properties. The Sb concentrations improve the crystallinity of the films through occupying the sulphur, indium, and other vacancy sites without affecting the structure of $MnSbInS_4$ thin films[50]. Further, at higher substrate temperature the size of the crystals formed on the surface is large enough to prevent surface defects and intrinsic defects, which is a good indication for better crystallinity of $MnSbInS_4$ thin films[51].

From Table 3, it can be clearly observed that increase in the film thickness reduces the transmittance of the film. As the film thickness increases the surface roughness and the density of localized states increases which reduces the transmittance value[52]. For the film thickness 768 nm, the transmittance is 62% Higher transmittance 80 % is noted for the film with the thickness of 617 nm. This is due to the increase in structural homogeneity and crystallinity lead to higher transmission[53].

The absorption coefficient (α) is calculated using the following equation[54].

$$\alpha = \frac{2.303}{t} \log\left(\frac{1}{T}\right) \quad \ldots (5)$$

where, T is the transmittance and t is the thickness of the film. The thickness of the films was measured by a stylus profilometer. The variation of absorption coefficient with substrate temperature (250-400 °C) is shown in Fig. 4 and Table 3.

From Table 3, it is observed that the value of the absorption coefficient of the material of the film decreases as the substrate temperature increases[55]. A

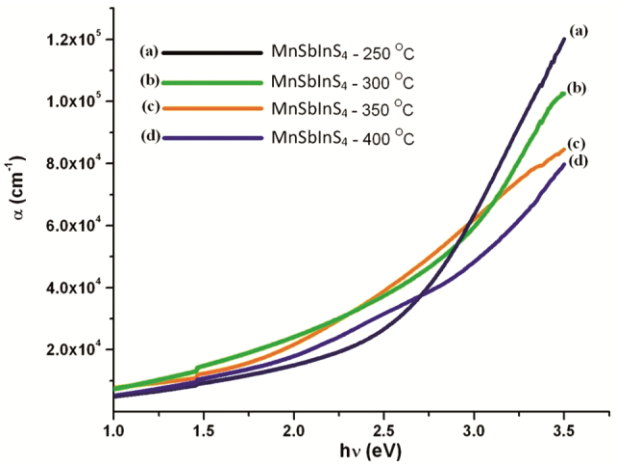

Fig. 4 — Variation of absorption coefficient (α) with band gap energy values (E_g) for $MnSbInS_4$ films prepared at various substrate temperatures: (a) 250 °C (b) 300 °C (c) 350 °C (d) 400 °C

higher value of α is obtained when the substrate temperature is at 250 °C (α = 1.22 x 10^5 cm^{-1}). This may be due to the presence of thermal lattice vibrations and imperfections in the grown films[56]. Further, the increase in the substrate temperature produces a significant effect on the energy of the absorption edge. It shifts the absorption edge to the longer wavelength (red shift), which is attributed to the growth of crystal grains and consequent decrease of quantum size effect[57]. The shift in the absorption edge towards the higher wavelength (red shift), is due to decrease in lattice strain with the increase of substrate temperature (Table 1). Moreover, the shift in the absorption edge towards the higher wavelength is due to the strong quantum confinements and enhancement in their surface area to volume ratio[58].

The extinction coefficient (K) is determined by using the relation[35].

$$K = \frac{\alpha \lambda}{4 \pi} \quad \ldots (6)$$

where, α is the absorption coefficient of the material of the film, λ is the wavelength of the incident light. The variation of the K with substrate temperature is presented in Table 3. From Table 3, it is observed that the absorption coefficient (α) and extinction coefficient (k) of the material of the film decrease

with increase in substrate temperature. This is attributed to the improvement in the crystallinity of the films with an increase in substrate temperature which leads to minimum imperfections[59].

3.4 Photoluminescence (PL) studies

Photoluminescence (PL) spectroscopy is a very efficient, contactless, non-destructive, widely used technique for the analysis of the optoelectronic properties of semiconductors, which requires very little sample manipulation. The main uses of photoluminescence are to understand the recombination mechanisms, identification of surface interface and impurity levels, band gap determination, assessment of the material quality and detection of defect states. The photoluminescence (PL) spectra of $MnSbInS_4$ thin films prepared at various temperatures are shown in Fig. 5. The PL spectra were recorded at room temperature with an excitation wavelength of 350 nm. From figure 5, several intense peaks are observed in the wavelength range 340-680 nm corresponding to blue, green, yellow, orange and red band emission. The intense peak corresponding to UV- region (394nm) is due to the band edge emission and other peaks in the Vis – IR regions are also due to the defect emissions[60,61]. Further, it is observed that the emission peak intensity increases with an increase of substrate temperature. The increase of peak intensity at higher substrate temperatures may result in the reduction of micro- strain and defect states as well as improvement in crystallite size, which could improve the crystallinity of the material of the film[62]. At the substrate temperature 400°C, a strong peak is observed in the wavelength range 600-650 nm centered at 628 nm (maximum emission) may be due to donar- acceptor pair transition (DAP) between a sulphur vacancy and an indium vacancy or manganese on an indium site[63-65]. Moreover, the PL studies play an important role in determining the exact energy levels of nanostructures of polycrystalline thin films[66].

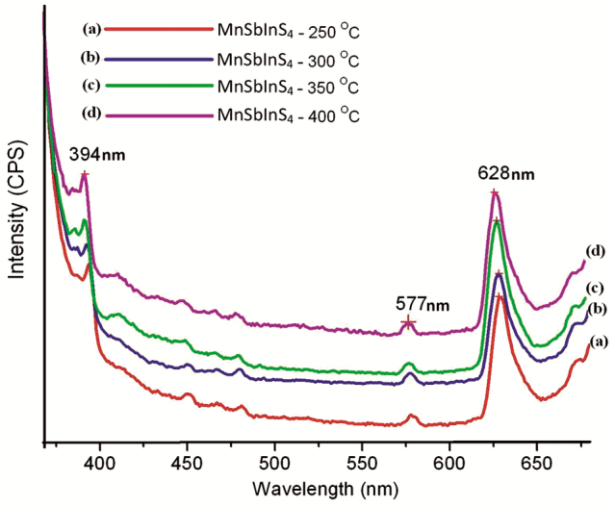

Fig. 5 — Photoluminescence spectra of MnSbInS4 films excited by 350 nm at various substrate temperatures: (a) 250 °C (b) 300 °C (c) 350 °C (d) 400 °C

3.5 Electrical studies

The resistivity of the film depends on several factors like preparation parameters, doping agents, variation in temperature and the dimension of the film. The electrical resistivity and conductivity of the deposited films are calculated by the following equations[67]:

$$\rho = 4.532 \left(\frac{V}{I}\right) t \qquad \ldots (7)$$

$$\sigma = \frac{1}{\rho} \qquad \ldots (8)$$

where, V is the Voltage in volts, I is the current in Ampere and t is the thickness of the film. The variation of electrical conductivity with substrate temperature for $MnSbInS_4$ thin film is shown in Fig. 6 and Table 4.

Table 4 — Variation of resistivity (ρ), conductivity (σ) and activation energy (E_a) of $MnSbInS_4$ thin films with substrate temperatures (250-400ºC).

Substrate temperature (°C)	Resistivity ρ (Ω m)	Conductivity σ $(\Omega\ m)^{-1}$	Activation Energy(E_a) eV
250	3.12×10^5	1.94×10^{-6}	0.247
300	7.80×10^4	1.35×10^{-5}	0.242
350	1.52×10^4	6.61×10^{-5}	0.225
400	4.77×10^3	2.12×10^{-4}	0.213

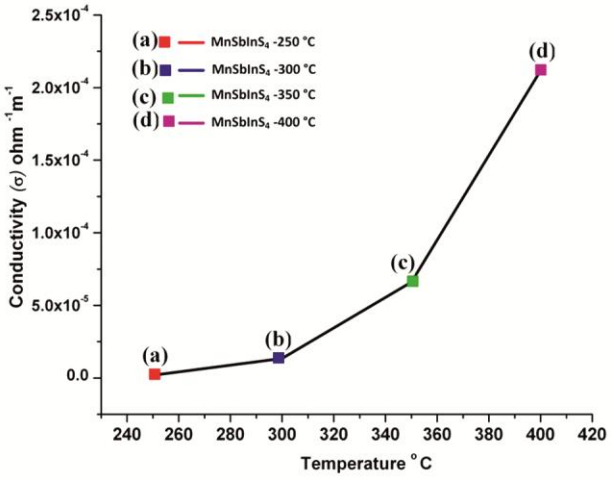

Fig. 6 — Variation of electrical conductivity of $MnSbInS_4$ thin films sprayed at different substrate temperature: (a) 250°C (b) 300°C (c) 350°C (d) 400 °C.

From Table 4, it is noted that the electrical conductivity increases with an increase of substrate temperature and supports the semiconducting nature of $MnSbInS_4$ thin films[68-72]. It is also noted that the conductivity is found to be 1.94 x 10^{-6} Ω^{-1} m^{-1} for the film deposited at 250°C and attains a maximum value of 2.12 x 10^{-4} Ω^{-1} m^{-1} for the film prepared at 400 °C. The increase in conductivity of the material of the films with substrate temperature is due to the growth of grain size (16.6-27.8 nm) and improvement in the crystallinity of the films[73]. This inference on the improvement of crystallinity of the films with increasing in substrate temperature is consistent with present FE-SEM and XRD results. The higher value of conductivity (low resistivity) at a higher temperature of $MnSbInS_4$ thin films exhibit the semiconducting property and find wide applications in the field of opto-electronics[74].

On the other hand, the resistivity (ρ) is found to be higher (3.12 x 10^5 Ω m) at 250°C than at 400°C (4.77 x 10^3 Ω m). The decrease in resistivity of the film at higher substrate temperature may be due to the presence of oxygen vacancies (from EDS spectrum) during the process of film growth[75,76]. These oxygen vacancies can act as electron donors and increase the free carrier concentration which greatly reduces the resistivity and increase the electrical conductivity of the film[77,78]. Further, the decrease in electrical resistivity of the film at higher substrate temperature is due to the improvement in crystallinity of the films which would increase the charge carriers, mobility and decrease the defect states[79]. The highest grain size (27.8 nm at 400°C) indicates the highest electrical conductivity and lowest resistivity of the film. Similar behaviour has been observed in the films of other materials[80,81]. In the case of larger grain films, the charge transport is predominant which results from the substantial improvement in the conductivity, whereas in the case of smaller grain films, the higher number of grain walls may act as low conductivity blockades[82]. Further, the increase in the grain size allows a decrease in electron scattering which leads to an increase in electrical conductivity[83].

The activation energy of the films for different substrate temperatures is calculated using the following relation[84].

$$E_a = 0.08625\, x\ slope \quad \ldots (9)$$

where, 0.08625 is the value of Boltzmann constant in e V. The E_a values are calculated by plotting a graph between log (ρ) and (1000/T) for the films deposited at different substrate temperatures (Fig 7) and they are presented in Table 4. From Table 4, the activation energy (E_a) values for 250, 300, 350 and 400 °C are 0.247, 0.242, 0.225 and 0.213 eV. It is noted that the activation energy decreases with an increase in the substrate temperatures (250-400 °C)[85]. This may be due to the increase of grain size and improvement in the crystallinity of the films (Table 1) at higher substrate temperature[79]. Further, the decrease in activation energy is due to the metal doping. The effect of doping is to eliminate the structural defects and dangling bonds which improve in the crystalline structure and this is clearly noticed from the XRD studies[86].

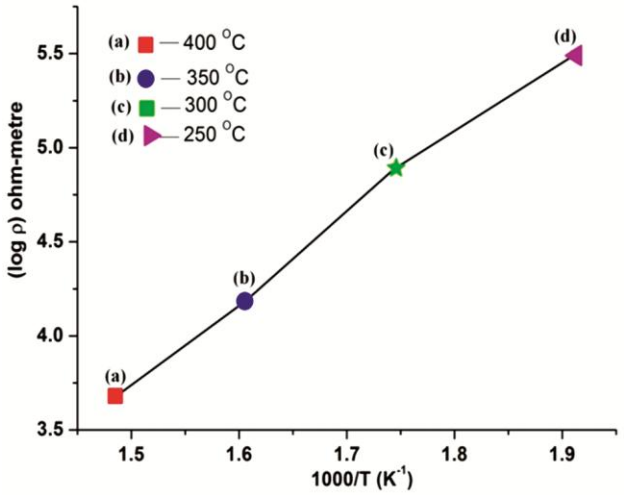

Fig. 7 — Variation of log (ρ) versus 1000/T (K^{-1}) for different substrate temperatures of $MnSbInS_4$ thin films. Substrate temperature: (a) 250 °C (b) 300 °C (c) 350 °C (d) 400 °C

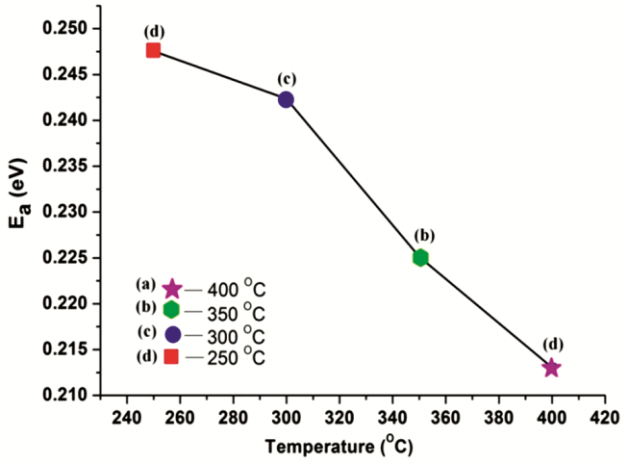

Fig. 8 — Variation of activation energy (E_a) of $MnSbInS_4$ thin films prepared at different substrate temperatures: (a) 250 °C (b) 300 °C (c) 350 °C (d) 400 °C

4 Conclusions

The $MnSbInS_4$ films are prepared on glass substrates by a simple chemical spray pyrolysis technique and their physical properties are investigated. The XRD analysis indicates that these films have cubic spinel structure with a grain size ranging between 16.8 and 28.2 nm. It is noted that the crystalline size increases with an increase of substrate temperature (250-400 °C). The increase in substrate temperature promotes the crystallite growth and improves the crystallinity of the films. Also, at a substrate temperature 250 °C, the EDS spectrum confirms the presence of Mn, In, S and Sb in the synthesized film. From the optical studies, it is noted that the transmittance percentage is increased with the increase in the substrate temperature. The improved optical transmittance at higher temperatures is due to the occupancy of Sb atoms in sulphur, indium, and other vacancy sites. It is also observed that the absorption coefficient and extinction coefficient of the material of the film decrease with the increase in the substrate temperature. This may be due to the improvement in structural homogeneity which leads to minimum imperfections. From the photoluminescence spectra, it is observed that the presence of a large number of defect states during the growth of the thin films results in a large number of emission peaks in the UV and Vis-IR regions. Analysis carried out by four-probe method indicates high value of electrical conductivity (2.12×10^{-4} $\Omega^{-1}m^{-1}$) is obtained by the film coated at 400°C, this predicts the semiconducting behavior of the prepared thin films. Therefore, it is very clear from the present work, the substrate temperature and metal doping play an important role in varying the physical property of the thin film, making it suitable for the use in optoelectronic devices.

Acknowledgement

The authors thanks the Bishop and Correspondent, CSI College of Engineering, CSI Coimbatore diosese, Tamilnadu – India for his constant encouragement and support.

References

1 Larramendi E M, Calzadilla O, Arias A G, Hernandez E & Garcia J R,*Thin Solid Films*, 389 (2001) 301.
2 Ubale A U, Sangawar V S & Kulkarni D K, *Bull Mater Sci*, 30 (2007) 147.
3 Ravichandran K & Philominathan P, *Appl Surf Sci*, 255 (2009) 5736.
4 Sonawane P S, Wani P A, Patil L A & Seth T, *Mater Chem Phys*, 84 (2004) 221.
5 Khefacha Z, Benzarti Z & Mnari M, *J Cryst Growth*, 260 (2004) 400.
6 Anuar K, Tan W T, Atan M S, Dzulkefly K A, Md Jelas H, Ho S M & Saravanan N, *J Ultra Chem*, 5 (2009) 21.
7 Maity R & Chattopadhyaya K K, *Sol Energy Mat Sol Cells*, 90 (2006) 597.
8 Mane R, Pathan H, Lokhande C & Han S, *Sol Energy*, 80 (2006) 185.
9 Niftiev N N, *Solid State Commun*, 92(1994) 781.
10 Kumar T P & Sankaranarayanan K, *Chalcogenide Lett*, 6 (2009) 617.
11 Yamaguchi K, Yoshoda T & Minoura H, *Thin Solid Films*, 354 (2003) 431.
12 Inov R & Desheva D, *Thin Solid Films*, 213 (1992) 230.
13 Chai B, Zeng P, Zhang X H, Mao J, Zan L & Peng T Y, *Nanoscale*, 4 (2012) 2372.
14 Naghavi N, Spierings S, Powalla M, Cavana B & Lincot D, *Prog Photovolt Res Appl*, 11 (2003) 437.
15 Madhusudhan Reddy M H & Chandorkar A N, *Thin Solid Films*, 349 (1999) 161.
16 Elangovan E & Ramamurthi K, *Appi Surf Sci*, 249 (2005) 183.
17 Tomakin M, Aitunbas M, Bacaksiz E & Celik S, *Thin Solid Films*, 520 (2012) 2532.
18 Nithyaprakash D, Ramamurthy M, Thirunavakarasu P, Balasubramaniam T, Chandrasekaran J & Maadeswaran P, *J Optoelec Biomedical Mater*, 1(2009) 42.
19 Sharma R K, Lakshmikumar S T, Gurmeet Singh & Rastogi A C, *Mater Chem Phys*, 92 (2005) 240.
20 Kamoun N, Belgacem S, Amoluk M, Bennaceur R, Bonnet J, Touhari F, Nouaoura M & Lassabatere L, *Appl Phys*, 89 (2001) 2766.
21 Guk M, Merschjann C, Bodner I, Tyborski T, Schedel-Niedrig T, Lux-Steiner M & Arushanov E, *Opt Mater*, 34 (2012) 915.
22 Lokhande C D, Ennaoui A, Patil P S, Giersig M, Diesner K, Muller M & Tributsch H, *Thin Solid Films*, 340 (1999) 18.
23 Fan B D, Wang H, Zhang Y C, Cheng J, Wang B & Yan H, *Mater Chem Phys*, 80 (2003) 44.
24 Fan D B, Wang H, Zhang Y C, Cheng J, Wang B & Yan H, *Sur Rev Lett*, 11 (2004) 27.
25 Gumus C, Ulutas C, Esen R, Ozkendir O M & Ufuktepe Y, *Thin Solid Films*, 492 (2005) 1.
26 Kanomata H & Kenako, *J Phy Soc Jpn*, 34 (1973) 554.
27 Taguchi H, *Solid State Commun*, 92 (1994) 635.
28 Mallika A N, Ramachandra R A, Sowri B K, Sujatha C & Reddy V, *Opt Mater*, 36 (2014) 879.
29 Battachacharyya S R & Pal A K, *Bull Mater Sci*, 31 (2008) 73.
30 Brown B J & Bates C W, *Thin Solid Films*, 188 (1990) 301.
31 Krunks M, Madarasz J, Hilltunen L, Mannonen M, Mellikov E & Niinisto L, *Acta Chemica Scandinavica*, 51 (1997) 294.
32 Krunks M, Mellikov E & Bijakina O, *Phys Sci*, T69 (1997) 189.
33 Farag M A, El-okr M, Mahani R M, Turky G M & Afify H H, *Int J Adv Eng Commun Sci*, 1 (2014) 1.
34 Ashour A, *Turk J Phys*, 27 (2003) 551.
35 Venkatachalam M & Sathe S K, *J Agricultural Food Chem*, 54 (2006) 4705.

36 Alili M & Kamoun N T, *J Mater Sci Mater Electron*, 25 (2014) 3840.
37 Muthukumaran S & Ashok K M, *Mater Lett*, 93 (2013) 223.
38 Rakesh V & Vaidyan V K, *J Opt Bio Mater*, 1 (2009) 281.
39 Jassim S A J, Zumaila A A R A & Waly G A A A, *Results Phys*, 3 (2013) 173.
40 Berg R S & Nasby R D, *J Vac Sci Technol*, 15 (1978) 359.
41 Scheer R, Alt M, Luck I & Lewerez H J, *Sol Energy Mater Sol Cells*, 49 (1993) 423.
42 Patil P S & Kadam L D, *Appl Surf Sci*, 199 (2002) 211.
43 Aldrin A, *Cochin University of Science and Technology*, (2004).
44 Moreh A U, Momoh M & Hamza B, *Int J Eng Sci Invent*, 2 (1) (2013) 48.
45 Bedia A, Bedia F Z, Aillerie M, Maloufi N & Benyoucef B, *Energy Procedia*, 74 (2015) 529.
46 Sivaraman T, Nagarathinam V S & Balu A R, *Res J Mater Sci*, 2 (2014) 6.
47 Naji I S, khudhid I H & Mohamaed H I, *Inter J Appl Innov Eng Manag*, 2 (2013) 556.
48 Kennedy A, Viswanathan K, Krishnamoorthy N & Pradeev raj K, *Mater Sci Semicond Proscess*, 48 (2016) 39.
49 Yamaguchi M & Arito M M M, *Mater Trans*, 45 (2004) 522.
50 Suriyanarayan N & Mahendran C, *Physica B*, 408 (2013) 62.
51 Raj M J, Sanjeeviraja C & Amalraj L, *J Asian Ceram Soc*, 4 (2016) 191.
52 Kumar N, Parihar U, Kumar R, Patel K J, Panchal C J & Padha N, *Am J Mater Sci*, 2 (2012) 41.
53 Mortezaali A, *Micro Electron Eng*, 151 (2016) 19.
54 Choi J Y, Kim K J, Yoo J B & Kim D, *Solar Energy*, 64 (1998) 41.
55 Mandal M, Choudhury S, Das C & Begum T, *Eur Sci J*, 10 (2014) 442.
56 Mott N & Davis E, *Electronic Process in Non-crystalline Materials, Second edition, University Press, Oxford*, 1979.
57 Kathalingam A, Magalingam T & Sanjeeviraja C, *Mater Chem Phys*, 106 (2007) 215.
58 Mortezuali A, Taheri O & Hossrui, *Microelectron Eng*, 151 (2016) 19.
59 Prathap P, Subbanah Y P V, Devika M & Ramakrishna R K T, *Mater Chem Phys*, 2-3 (2006) 375.
60 Dieti T, Shno H, Matsukura F, Cibert J & Ferrand D, *Appl Surf Sci*, 287 (2000) 1019.
61 Tam K H, Cheung C K O, Leung Y H, Djurisic A B, Ling C C, Beling C D, Fung S, Kwok W M, Chan W K, Phillips D L, Ding L & Ge W K, *J Phys Chem B*, 110 (2006) 20865.
62 Singh S, Srinivasa R S & Major S S, *Thin Solid Films*, 515 (2007) 8718.
63 Van G J, Versluys J, Poelman D, Verschraegen J, Burgelman M & Chauws P, *Thin Solid Films*, 511-512 (2006) 304.
64 Eberhardt J, Metzner H, Goldhahn R, Hudert F, Reishlohner U, Hulsen C, Cieslak C J, Haha T H, Gossla M, Oietz A, Gobsch G & Witthuhn W, *Thin Solid Films*, 480-481 (2006) 415.
65 Nanu M, Schoonman J & Goossens A, *Thin Solid Films*, 193 (2004) 451.
66 Magendran C & Suriyanarayanan N, *Physica B*, 405 (2010) 2009.
67 Panta G P & Subedi D P, *J Sci Eng Tech*, 8 (2012) 31.
68 Sato H, Minami T, Takata S & Yamada T, *Thin Solid Films*, 236 (1993) 27.
69 Chen X, Wu N J, Smith L & Ignatiev A, *Appl Phys Lett*, 84(14) (2004) 2700.
70 Kadam L D, Bhosale C H & Patil P S, *Turkish J Phys*, 21 (1997) 1037.
71 Adler D, Tjeng L H, Voogt F C, Hibura T, Sawatzky G A, Chen C T, Vogel J, Sacchi M & Iacobucci S, *Phys Rev B:Condensed Matter Mater Phys*, 57 (1998) 11623.
72 Davazoglou D, Leveque G & Dorradieu A, *Sol Energy Mater*, 17 (1988) 379.
73 Ubale A U & Kulkarni R K, *Indian J Appl Phys*, 44 (2006) 254.
74 Panday P K, Bhave N S & Kharat R B, *Indian J Appl Phys*, 44 (2006) 281.
75 Carroll A F & Slack L H, *J Electrochem Soc*, 123 (1976) 1889.
76 Mulla I S, Soni A S, Rao V J & Sinha A P B, *J Mater Sci*, 21 (1986) 1280.
77 Fan J C & Goodenough B, *J Appl Phys*, 48 (1977) 3524.
78 Choudhury M G M, Kao J S, Lai G R & Ali A G M R, *Indian J Pure Appl Phys*, 41 (2003) 362.
79 Viswakarma R J, *J Theor Appl Phys*, 9 (2015) 185.
80 Parameshwari P, Sashidhara B & Gopalakrishna, *Arch Phys Res*, 3 (2012) 441.
81 Xinon Q, Wang W & Sunchen L, *Solid State Commun*, 152 (2011) 332.
82 Ravichandran K, Muruganatham G, Sakthivel B & Philominathan P, *J Ovonic Res*, 5 (2009) 63.
83 Houng B, His C S, Zhang B Y & Shen L F, *Vacuum*, 83 (2009) 534.
84 Hassan A J, *J Mod Phys*, 5 (2014) 2184.
85 Ragupathi, George J & Menon C S, *Indian J Pure Appl Phys*, 43 (2005) 620.
86 Kaleel S G, Suhail M H & Yasser F M, *Int J Emer Tech Adv Eng*, 4 (2014) 613.